CHARACTERIZATION OF SUPERCONDUCTING SAMPLES WITH SIC SYSTEM FOR THIN FILM DEVELOPMENTS: STATUS AND RECENT RESULTS*

G. Eremeev†, L. Phillips, C.E. Reece, A.-M. Valente-Feliciano, B.P. Xiao‡,
Thomas Jefferson National Accelerator Facility, Newport News, U.S.A.

Abstract

Within any thin film development program directed towards SRF accelerating structures, there is a need for an RF characterization device that can provide information about RF properties of small samples. One of the RF characterization devices at Jefferson Lab is Surface Impedance Characterization (SIC) system. The data acquisition environment for the system has recently been improved to allow for automated measurement, and the system has been routinely used for characterization of bulk Nb, films of Nb on Cu, MgB_2, NbTiN, Nb_3Sn films, etc. We present some of the recent results that illustrate present capabilities and limitations of the system.

INTRODUCTION

The development of new materials as well as understanding current limiting loss mechanisms and material behavior in RF fields calls for an RF system capable of high resolution ($\propto$ 1 nΩ) surface resistance measurement device with a high magnetic field reach (greater than 200 mT). The system also should allow for a fast turn around and host sample sizes that can be accommodated in the standard material characterization systems. Over the years a number of sample RF characterization systems have been developed [1–8], but none of them has been able to match the resolution and field reach of the best SRF cavities. Still, RF characterization host cavities are widely used to characterize superconducting samples, and a number of systems are under development [9–11].

One of sample RF characterization systems at Jefferson Lab is Surface Impedance Characterization (SIC) system. The system has been shown in the past to resolve RF surface resistance on the order of 1 $\mu\Omega$ and a field reach on the order of 10 mT at 2 K. Presently, the system is been heavily used for niobium on copper thin film development and new material characterization in RF fields. This paper is the status report of the system: we summarize the experimental setup and characterization method, and show some of the recent results to illustrate SIC's capabilities.

EXPERIMENTAL SETUP

SIC system employs a cylindrical cavity loaded with high permittivity sapphire to reduce the TE_{011} frequency to 7.4 GHz [12, 13]. A flat two inch sample under investigation forms a part of RF structure, but is thermally decoupled from the rest of the RF cavity, so that the RF cavity remains at the helium bath temperature (typically 2 K) while the temperature of the sample is varied. The dissipation induced by RF field on the sample is derived via the power compensation technique:

$$P_{RF}(H_{peak}, T_{sample}) = P_{heater}^{H=0;T=T_{sample}} - P_{heater}^{H=H_{peak};T=T_{sample}} \quad (1)$$

where $P_{heater}^{H=0;T=T_{sample}}$ is the heater power needed to maintain the temperature of the sample at $T = T_{sample}$ with zero RF field in the cavity, and $P_{heater}^{H=H_{peak};T=T_{sample}}$ is the heater power needed to maintain the temperature of the sample at $T = T_{sample}$ with RF field in the cavity such that $H = H_{peak}$ on the sample. The average RF surface resistance of the sample can then be defined as:

$$R_{RF}(H_{peak}, T_{sample}) = \frac{P_{RF}(H_{peak}, T_{sample})}{k \cdot H_{peak}^2} \quad (2)$$

, where k = 3.70·10^7 $\frac{W}{\Omega T^2}$ = 5.84·10^{-5} m^2 is a constant related to the surface area of the sample exposed to RF fields and found with numerical simulations, and H_{peak} is the peak magnetic field on the surface of the sample.

The first part of SIC measurement is the measurement of loaded quality factor of the cavity as a function of the sample temperature using a network analyzer. Presently, Agilent's FieldFox N9915A, connected to the network for data communication, is used for loaded Q measurement. Labview program automatically collects the data from all instruments, and controls the temperature of the sample. The program sets the temperature controller's set temperature according to the user-defined temperature list, waits for the sample's temperature to stabilize, tracks the resonant frequency and keeps the network analyzer's frequency sweep centered on the resonant frequency. Once the sample's temperature is stable and within 3 mK of the set temperature, Q loaded measurement is initiated. The Q loaded is measured with 3 dB technique for several frequency spans, from which average loaded quality factor and the standard deviation are determined. A typical Q_L versus temperature result is shown in Fig. 1 with bars representing random error.

* Authored by Jefferson Science Associates, LLC under U.S. DOE Contract No. DE-AC05-06OR23177. The U.S. Government retains a non-exclusive, paid-up, irrevocable, world-wide license to publish or reproduce this manuscript for U.S. Government purposes.

† grigory@jlab.org
‡ presently with BNL, Upton, New York, U.S.A.

ISBN 978-3-95450-143-4

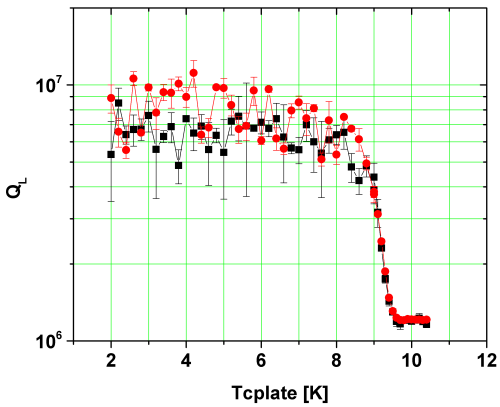

Figure 1: A representative measurement of loaded quality factor as a function of temperature is shown in this plot. One can see loaded quality factor of about 10^7 at lower temperatures. The quality factor drops as the sample temperature approaches the superconducting transition temperature of the sample. The red and black data points are data for two subsequent measurements without disassembly. The bars show a random error deduced from several frequency scans with the network analyzer.

After the network analyzer measurements a standard PLL RF system is connected to the cavity and the surface resistance is measured using the power compensation technique, Fig. 2. The stored energy, and hence RF field, is derived from the PLL measured power levels and the loaded quality factor measured with the network analyzer.

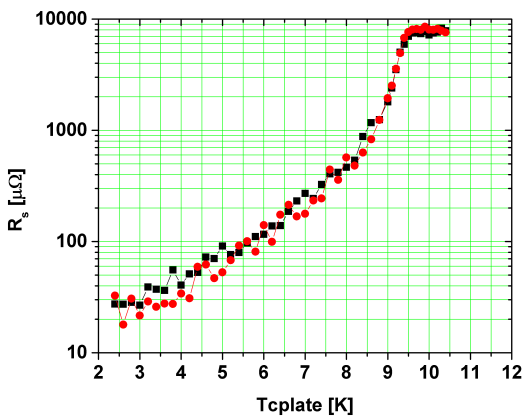

Figure 2: A representative measurement of RF surface resistance. The red and black data points are data for two subsequent measurement at different power levels without disassembly.

The output of frequency modulated RF source is amplified by a 1 Watt RF amplifier, which generates peak magnetic fields of about 1 mT on the sample surface. 200 Watt amplifier has been procured to extend field reach and its implementation is foreseen.

RESULTS AND DISCUSSION

Thin Film ECR Films Results

SIC system has been used heavily to characterize niobium films on copper coated in electron cyclotron resonance (ECR) system at Jefferson Lab. In Fig. 3 we show the surface resistance as a function of temperature for several ECR Nb films coated with different ion energies (124 eV, 154 eV, 184 eV, 214 eV, 244 eV, 264 eV). The thickness of the films ranges from 0.9 μm to 2.5 μm [14, 15].

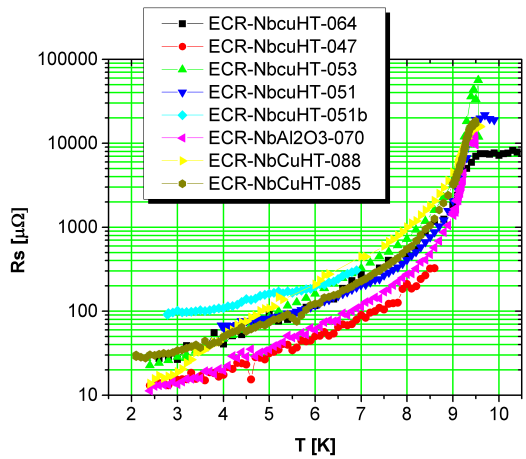

Figure 3: In this plot recent surface resistance measurements of niobium thin film coated on copper substrates with ECR technique are presented. The thickness of the films ranges from 0.9 μm to 2.5 μm [14, 15].

Nb_3Sn Results

We used a Nb chamber loaded with niobium samples, Sn, and $SnCl_2$ to produce Nb samples coated with Nb_3Sn. Two flat Nb samples in the chamber were fine grain and large grain niobium samples. After the coating the samples had visually different surface: the fine grain sample had a uniform coating, whereas the large grain sample has surface features, commonly referred as "droplets", similar to those observed in other studies. Surface resistance of both samples was measured in SIC system, Fig. 4. The large grain sample with "droplets" exhibits residual surface resistance of about 1 mΩ, which is almost two orders of magnitude higher than that of the fine grain sample with uniform coating, which exhibits residual surface resistance of about 20 $\mu\Omega$.

NbTiN Results

SIC measurements are being done on the thin film multilayer samples. Two NbTiN films have been recently measured. One of the samples was NbTiN thin film deposited on a bulk niobium sample with AlN dielectric interlayer. The bulk Nb substrate is a single crystal that was mechanically polished, electropolished and etched with BCP [1:1:4] to remove the final 10 μm. The sample was baked at 600 °C for 24 h and then coated and annealed for 4h at

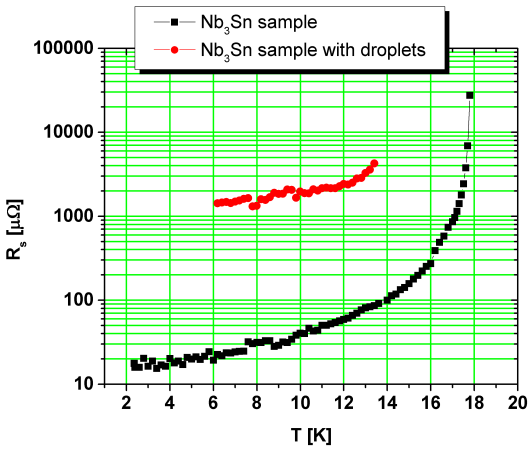

Figure 4: Surface resistance measurements of Nb_3Sn coated on large grain and fine grain samples are presented. The red circles are data for a Nb_3Sn coated large grain sample. The black squares are data for a Nb_3Sn coated fine grain sample.

450 °C. The NbTiN and AlN layers are respectively 200 nm and 20 nm thick. The NbTiN layer exhibit the δ-phase as measured with Bragg-Brentano (XRD). The other thin film NbTiN was coated on thin film Nb deposited with electron cyclotron resonance deposition system on bulk Cu sample with AlN and Al_2O_3 dielectric interlayers. The NbTiN/AlN structure deposited on an ECR Nb film on a-Al_2O_3 was coated with the same parameters as the one on the bulk sample. The quality factor measurements are shown in Fig. 5[top]. Both samples exhibit two transitions, one corresponding to NbTiN layer and the other to underlying superconducting Nb layer. The depression in the critical temperature for the multilayer structure on ECR sample is most likely due to the diffusion of oxygen from the oxide layer into the film. The surface resistance measurements on these samples are still under way, but the film coated onto bulk niobium sample has higher quality factor at all temperatures, which implies lower surface resistance. In Fig. 5[bottom] we plotted the derivative of the RF transmission s21 as a function of temperature. We use the s21 derivative plots to infer the transition temperatures and transition temperature variation within the film.

CONCLUSIONS

Surface impedance characterization (SIC) cavity has been routinely used to characterize flat two inch diameter samples coated with various materials. Recent automation of data acquisition allowed for a higher capture rate and autonomous measurement. In this contribution we presented some measurements of thin film niobium, thick film Nb_3Sn, and superconductor-insulator-superconductor sample that illustrated the setup, its applications, and the capabilities of the system. The present challenges towards extending system capabilities include the increase in the field reach, understanding of the quality factor limitations and high residual resistance in some samples.

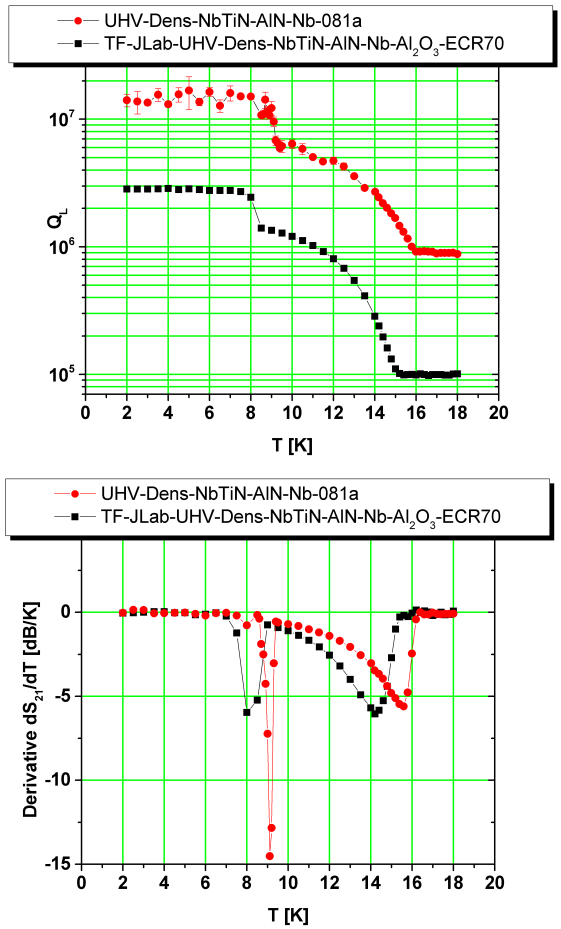

Figure 5: In the top plot the Q_L vs. T data is presented for two NbTiN films: the red circles correspond to the film coated on niobium with AlN dielectric interlayer; the black squares correspond to the film coated on Nb on Cu with AlN and Al_2O_3 dielectric interlayers. In the bottom plot the derivative of s21 transmission is presented. The data illustrates transition temperature and transition temperature variation for both NbTiN and underlying Nb films. The depression in the critical temperature for the multilayer structure on ECR sample is most likely due to the diffusion of oxygen from the oxide layer into the film.

ACKNOWLEDGEMENT

We would like to thank Jim Follkie, Danny Forehand, Tom Goodman, Teena Harris, Pete Kuchnick, Roland Overton, and Era Perry for the help with the cavity treatments, test preparations, and cooldowns. We would like to thank P. Kneisel who kindly provided niobium chamber, Sn, and $SnCl_2$ for Nb_3Sn deposition.

REFERENCES

[1] L. Phillips, G. K. Davis, J. R. Delayen, J. P. Ozelis, T. Plawski, H. Wang, G. Wu, Proc. of the 12th SRF Workshop, Ithaca, NY, U.S.A. (2005).

ISBN 978-3-95450-143-4

[2] B. Xiao, R.L. Geng, M.J. Kelley, F. Marhauser, H.L. Phillips, C.E. Reece, H. Wang, Proc. of the 14th SRF Conference, Berlin, Germany (2009) p.305.

[3] M.Ribeaudeau, JP.Charrier, S.Chel, M.Juillard, M.Fouaidy, M.Caruette, Proc. of EPAC, Stockholm, Sweden (1998) p. 1873.

[4] G. Martinet, S. Blivet, N. Hammoudi, M. Fouaidy, Proc. of the 14th SRF Conference, Berlin, Germany (2009) p.293.

[5] E. Mahner, S. Calatroni, E. Chiaveri, E. Haebel, and J. M. Tessier, Rev. Sci. Instrum. 74(7) (2003).

[6] T. Junginger, W. Weingarten, and C. Welsch, Proc. of SRF, Berlin, Germany (2009) p.130.

[7] C. Liang, L. Phillips, and R. Sundelin, Rev. Sci. Instrum. 64(7) (1993) p.1937.

[8] G. Ciovati, J. Mondal, P. Kneisel, G.R. Myneni, M. Morrone, R. Bundy, B. Clemens, T. Elliott, G. Slack, L. Turlington, Proc. of the 13th SRF Workshop, Beijing, China (2007) TUP01.

[9] D.L. Hall, M. Liepe, I.S. Madjarov, K. McDermott, N.R.A. Valles, THP038, these proceedings.

[10] R. Kleindienst, J. Knobloch, O. Kugeler, TUP074, these proceedings.

[11] C. Baumier, G. Martinet, J.-C. Villegier, C. Antoine, WEIOC02, these proceedings.

[12] B. P. Xiao, C. E. Reece, H. L. Phillips, R. L. Geng, H. Wang, F. Marhauser, and M. J. Kelley, Rev. Sci. Instrum. 82, 056104 (2011).

[13] B. P. Xiao, C. E. Reece, H. L. Phillips, R. L. Geng, H. Wang, F. Marhauser, and M. J. Kelley, Rev. Sci. Instrum. 83, 124905 (2012).

[14] A.-M. Valente-Feliciano, G.V. Eremeev, L. Phillips, C.E. Reece , J.K. Spradlin, TUP079, these proceedings.

[15] A.-M. Valente-Feliciano, G.V. Eremeev, L. Phillips, C.E. Reece, X. Zhao, J.K. Spradlin, TUP080, these proceedings.

ISBN 978-3-95450-143-4